30. F. Y. Chu and T. Oka, *J. Appl. Phys.* **46**, 1204 (1975).
31. D. N. Travis, J. L. McGurk, D. McKeown, R. E. Denning, *Chem. Phys. Lett.* **45**, 287 (1977).
32. D. Pritchard, J. S. Muenter, B. J. Howard, *ibid.* **135**, 9 (1987).
33. M. D. Marshall, A. Charo, H. O. Leung, W. Klemperer, *J. Chem. Phys.* **83**, 4924 (1985).
34. D. Ray, R. L. Robinson, D.-H. Gwo, R. J. Saykally, *ibid.* **84**, 1171 (1986); R. L. Robinson, D.-H. Gwo, D. Ray, R. J. Saykally, *ibid.* **86**, 5211 (1987).
35. H. S. Gutowsky, T. D. Klots, C. Chuang, C. A. Schmuttenmaer, T. Emilsson, *ibid.*, p. 569; T. D. Klots, C. Chuang, R. S. Ruoff, T. Emilsson, H. S. Gutowsky, *ibid.*, p. 5315.
36. S. E. Novick, P. B. Davies, T. R. Dyke, W. Klemperer, *J. Am. Chem. Soc.* **95**, 8547 (1987).
37. A. E. Barton, A. Chablo, B. J. Howard, *Chem. Phys. Lett.* **60**, 414 (1979).
38. K. W. Jucks *et al.*, *J. Chem. Phys.* **88**, 2185 (1988).
39. R. W. J. Wyckoff, *Crystal Structures* (Wiley-Interscience, New York, 1963), vol. 1.
40. G. T. Fraser, A. S. Pine, W. J. Lafferty, R. E. Miller, *J. Chem. Phys.* 87, 1502 (1987).
41. Z. S. Huang and R. E. Miller, in preparation.
42. S. H. Suck, J. L. Kassner, Jr., Y. Yamaguchi, *Appl. Opt.* **18**, 2609 (1979).
43. W. Burroughs, *New Sci.* 79, 544 (1978).
44. E. Huler and A. Zunger, *Chem. Phys.* **13**, 433 (1976).
45. O. Matsuoka, E. Clementi, M. Yoshimine, *J. Chem. Phys.* **64**, 1351 (1976); K. S. Kim, M. Depuis, G. C. Lie, E. Clementi, *Chem. Phys. Lett.* **131**, 451 (1986).
46. T. R. Dyke, K. M. Mack, J. S. Muenter, *J. Chem. Phys.* **66**, 498 (1977); J. A. Odutola, T. R. Dyke, *ibid.* 72, 5062 (1980).
47. L. H. Coudert, F. J. Lovas, R. E. Svenram, J. T. Hovgen, *ibid.*, in press.
48. R. H. Page, J. G. Frey, Y. R. Shen, Y. T. Lee, *Chem. Phys. Lett.* **106**, 373 (1984).
49. D. F. Coker, R. E. Miller, R. O. Watts, *J. Chem. Phys.* **82**, 3554 (1984).
50. R. S. Ruoff, T. D. Klots, C. Chuang, T. Emilsson, H. S. Gutowsky, paper presented at the 42nd Symposium on Molecular Spectroscopy, Ohio State University, 1987.
51. K. W. Jucks and R. E. Miller, *J. Chem. Phys.*, in press.
52. M. Kofranek, H. Lischka, A. Karpfen, *Mol. Phys.* **62**, 1519 (1987).
53. J. A. Beswick and J. Jortner, *Chem. Phys. Lett.* **49**, 13 (1977).
54. G. E. Ewing, *J. Chem. Phys.* 71, 3143 (1979).
55. A. C. Peet, D. C. Clary, J. M. Hutson, *Chem. Phys. Lett.* **125**, 477 (1986); *Faraday Discuss. Chem. Soc.* **82**, 327 (1986).
56. M. P. Casassa *et al.*, *Faraday Discuss. Chem. Soc.* **82**, 251 (1986).
57. D. S. King, in *Structure and Dynamics of Weakly Bound Molecular Complexes*, A. Weber, Ed. (Reidel, Dordrecht, 1987), p. 593.
58. Z. S. Huang, K. W. Jucks, R. E. Miller, *J. Chem. Phys.* **85**, 6905 (1986).
59. K. W. Jucks and R. E. Miller, *ibid.* **87**, 5629 (1987).
60. D. C. Dayton and R. E. Miller, *Chem. Phys. Lett.* **143**, 181 (1988).
61. C. M. Lovejoy, D. D. Nelson, Jr., D. J. Nesbitt, *J. Chem. Phys.* **87**, 5621 (1987).
62. B. A. Wofford, M. W. Jackson, J. W. Bevan, W. B. Olson, W. J. Lafferty, *ibid.* **84**, 6115 (1986).
63. K. L. Busarow *et al.*, *Chem. Phys. Lett.* **141**, 289 (1987).
64. I am grateful to my students K. W. Jucks, Z. S. Huang, and D. C. Dayton for their enthusiasm and hard work in carrying out many of the experiments discussed here. This research was supported by the National Science Foundation (CHE-86-03604) and the Sloan Foundation.

Theoretical Studies of the Energetics and Dynamics of Chemical Reactions

THOM H. DUNNING, JR., LAWRENCE B. HARDING, ALBERT F. WAGNER,
GEORGE C. SCHATZ,* JOEL M. BOWMAN†

Computational studies of basic chemical processes not only provide numbers for comparison with experiment or for use in modeling complex chemical phenomena such as combustion, but also provide insight into the fundamental factors that govern molecular structure and change which cannot be obtained from experiment alone. We summarize the results of three case studies, on HCO, $OH + H_2$, and $O + C_2H_2$, which illustrate the range of problems that can be addressed by using modern theoretical techniques. In all cases, the potential energy surfaces were characterized by using ab initio electronic structure methods. Collisions between molecules leading to reaction or energy transfer were described with quantum dynamical methods (HCO), classical trajectory techniques (HCO and $OH + H_2$), and statistical methods (HCO, $OH + H_2$, and $O + C_2H_2$). We can anticipate dramatic increases in the scope of this work as new generations of computers are introduced and as new chemistry software is developed to exploit these computers.

DURING THE PAST DECADE THE ABILITY OF THEORETICAL chemists to address important chemical problems has been significantly enhanced by advancements in computer technology. In 1977 the first supercomputer was introduced by Cray Research, Inc.; unfortunately, the chemistry community had only limited access to these powerful computers. In 1981 the first minisupercomputer was introduced by Floating Point Systems, Inc. The FPS-164 offered a tenth of the power of a Cray 1 supercomputer at the cost of a minicomputer (*1*); because of its speed and cost-effectiveness, the FPS-164 found widespread use in chemistry. More recently, chemists have gained access to supercomputers at the national supercomputer centers sponsored by the National Science Foundation and the U.S. Department of Energy.

During this same period revolutionary advances were made in theoretical methodology and computer algorithms for chemical computations. These developments—for example, the implementation of efficient configuration interaction (CI) algorithms based on the unitary group formalism (*2*), the development of effective many-body perturbation theory and coupled cluster techniques (*3*), and the derivation and coding of efficient techniques for computing energy derivatives (*4*) in ab initio electronic structure theory—have

---

The authors are at the Theoretical Chemistry Group, Chemistry Division, Argonne National Laboratory, Argonne, IL 60439.

*Permanent address: Department of Chemistry, Northwestern University, Evanston, IL 60201.
†Permanent address: Department of Chemistry, Emory University, Atlanta, GA 30322.

Fig. 1. Contour plot of the H + CO potential energy surface for $R_{CO} = 2.25a_0$ (0.119 nm). The thick solid curve is the zero-energy contour, solid curves denote positive contours, and dashed ones negative contours; the interval between contours is 5 kcal/mol. Y and Z refer to the in-plane coordinates of the hydrogen atom.

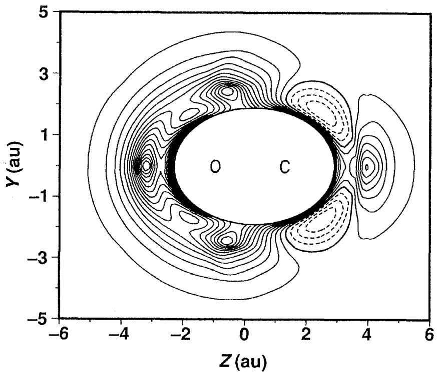

also greatly enhanced our ability to realistically describe molecular systems. Because of the advances in both chemistry software and computer hardware, theoretical chemistry has now become an indispensable component of many modern research programs in the chemical sciences. Theoretical studies provide insights into the details of molecular structure and dynamics that simply cannot be obtained from experiment alone. Furthermore, large-scale computer simulations can provide numerical data difficult to obtain in the laboratory.

In this article, we discuss some of the applications that we have been involved in recently that illustrate the capabilities of modern theoretical chemistry methods for describing the energetics and dynamics of elementary chemical reactions. All of these applications involve reactions of relevance to combustion chemistry, but interest in these reactions goes well beyond this area. Studies of chemical reactivity are, of course, a research focus in a number of other theoretical groups. Although a review of this body of work is beyond the scope of this article, we would be remiss if we did not note the intense theoretical work on the F + H_2 reaction, a prototypical chemical reaction that has long been the subject of detailed theoretical and experimental studies (*5*). Recently, in an attempt to determine an accurate barrier for this reaction, large-scale ab initio calculations have been reported by the groups at the University of California, Berkeley (*6*), the University of Minnesota (*7*), and the NASA Ames Research Center (*8*). This goal has proven challenging indeed, with the bare calculations yielding barriers of ~3 kcal/mol, whereas the experimental data appear to require a barrier of 1 to 1½ kcal/mol. Although the general features of the F + H_2 reaction are well understood, this is not the case for many other reactions. As an example of the important role that theory can play in providing a basic understanding of molecular reactivity, we note the studies of the chemistry of the technologically important silicon species recently reviewed by Gordon and co-workers (*9*).

To model chemical reactions ab initio we must first determine the interactions between the atomic and molecular species involved. These interactions define a potential energy hypersurface (PES) of dimension ($3N - 6$), where N is the number of atoms. We must then determine the motion of the nuclei on this PES, properly choosing parameters such as the translational energies of the reactants to simulate the experiment of interest. To calculate the PES, we solve the electronic Schrödinger equation using basis set expansion techniques. The changes that occur in the electronic structure of a molecular system as the reaction proceeds from reactants through the transition state to products are substantial. To describe these changes, our approach includes the following three elements: (i) the use of large basis sets to provide the flexibility needed to describe the variations in the electron distribution; (ii) the use of multiconfiguration self-consistent field wave functions to provide a consistent description of the reactants, transition state, and products; and (iii) the inclusion of electron correlation to provide quantitative predictions of the reaction energetics. With this approach we can study reactions with as many as five or six atoms with errors of just a few kilocalories per mole in the predicted reaction energetics.

The methods used to describe nuclear motion fall into several categories depending on the nature of the problem being described. Vibrational-rotational bound states of molecules are often determined by using methods analogous to those used to describe electronic structure. Collisions between molecules leading to reaction or energy transfer are usually described with classical trajectory techniques, although in favorable cases we can use exact quantum scattering methods. For bimolecular and unimolecular reaction rates, it is also possible (and often necessary) to use statistical methods such as transition state theory (TST) and RRKM theory. Trajectory and statistical methods can provide an accurate description of many dynamical processes, and, moreover, there is now a substantial body of experience concerning the applicability of these approaches under a variety of circumstances. As a consequence, the reliability of the results so obtained can often be accurately estimated.

The specific systems we will consider here are: (i) the formyl radical (HCO); (ii) the reaction of hydroxyl radical with molecular hydrogen, OH + H_2; and (iii) the reaction of oxygen atom with acetylene, O + C_2H_2. HCO is the simplest of the three systems and can be treated at the highest level of sophistication; a global PES has been computed, the vibrational levels of HCO have been calculated, and statistical, classical, and quantum dynamics studies of H + CO collisions have been, or are being, performed. The OH + H_2 reaction represents a system of intermediate complexity for which it is still possible to develop a global PES and determine the detailed dynamics, but for which the interpretation of the results is greatly facilitated by examining the properties of the PES near the minimum energy path leading from reactants to products. The O + C_2H_2 reaction is a more complex system where just the process of mapping out reaction paths is a significant challenge. In this case statistical theories that require information only on critical regions of the PES are the only practical tools for predicting reaction rates.

The H + CO System

Interest in the physics and chemistry of the H-CO system is far ranging. In astrophysics, very low energy, rotationally inelastic collisions of hydrogen atoms with carbon monoxide are of importance in establishing the rotational temperature of CO in interstellar clouds. For this process, the anisotropy of the long-range part of the potential is most important, and this has been determined semiempirically and used in quantum scattering calculations by several groups (*10*). Molecular beam studies, as well as theoretical studies focusing on the long-range part of the potential, have also been reported (*10, 11*).

At thermal energies and higher, the recombination of hydrogen atoms and carbon monoxide to form HCO and of the dissociation of HCO to these species are important in hydrocarbon combustion. The rates for both processes have been measured experimentally (*12, 13*), although not at the temperatures characteristic of flames ($T \approx 2500$ K). In addition, both RRKM (*13, 14*) and quantum scattering (*15, 16*) calculations have been reported. The portion of the potential describing the HCO radical and the barrier to its formation are of critical importance in these processes.

At hyperthermal energies, inelastic (vibrational, rotational) transitions in CO induced by collision with hot hydrogen atoms have been measured by several groups (*17*) and modeled by classical trajectory calculations (*18*). These experiments probe the short-

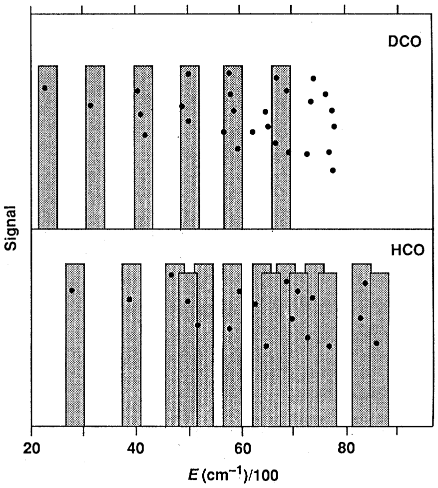

Fig. 2. The calculated and observed vibrational levels of the formyl radical, HCO. The experimental results are indicated by rectangles, of width 200 cm^{-1}, which corresponds to the experimental uncertainty in the vibrational energies. The calculated energies are represented by solid circles. The levels of HCO above 8000 cm^{-1} are resonances.

range, repulsive part of the potential corresponding to both the stable HCO isomer and the metastable HOC isomer. Finally, the spectral properties of HCO (and DCO) have been examined by several groups (*19–21*). These studies examine in detail the bound region of the HCO PES.

Calculation of a global PES for H + CO. The two most important inputs for an ab initio electronic structure calculation of a PES are the form of the many-electron wave function and the one-electron basis set used to expand the wave function. For HCO a basis set was chosen that provided two functions to describe each of the occupied atomic orbitals augmented with the first set of polarizations functions; the latter functions are needed to describe the deformation of the electronic density resulting from molecular formation and to properly treat electron correlation. With this basis set, CI calculations were performed including all single and double excitations from the Hartree-Fock (HF) wave function augmented with an estimate of the contribution of higher order excitations (*22*). This wave function accounts for the most important effects of electron correlation.

To map out a global PES for HCO, calculations were performed at approximately 2000 geometries (*21*). A small, but important, empirical correction was added to the ab initio surface to match the experimental activation energy and exothermicity for the addition reaction and to match the observed CH stretching frequency of the HCO radical. The resulting energies were then represented by a three-dimensional (3-D) spline function for use in the vibrational and dynamical calculations discussed below.

A 2-D slice through the 3-D surface of HCO (Fig. 1) shows minima that correspond to both the HCO and HOC isomers as well as transition states for addition of H to CO to form each of the isomers and a 1,2-hydrogen migration transition state for interconverting the two isomers. The HCO minimum is shallow, but bound relative to H + CO by 16 kcal/mol, whereas the HOC minimum is predicted to be metastable, that is, bound but lying 20 kcal/mol above H + CO.

Vibrational spectra of HCO (DCO) and HOC (DOC). The HCO PES was used to calculate all of the bound vibrational states of nonrotating HCO and DCO as well as some metastable states of the high-energy isomers, HOC and DOC (*21*). These variational calculations used the normal-coordinate Watson Hamiltonian and expanded the vibrational wave functions in a direct-product, harmonic-oscillator basis set. For the largest basis set considered, the energy eigenvalues are believed to be converged to 1 cm^{-1} or less for all but the two highest energy states of HCO (out of a total of 15) and all but the highest 6 states of DCO (out of a total of 28).

The results of these calculations are compared with the photodetachment experiments of Murray *et al.* (*20*) in Fig. 2. In these experiments the weakly bound electron in the HCO$^-$ (DCO$^-$) anion was photodetached by 488-nm laser light to form HCO in various (vibrational, rotational) states. The resolution of the electron energy analyzer together with the lack of rotational state selection of the anion resulted in a vibronic linewidth of about 200 cm^{-1}. First, consider the comparison for HCO. A total of 12 states were observed below the dissociation energy. However, the experimental spectrum is congested and badly overlapped at higher energies. In fact, three additional states predicted to lie below the dissociation limit were not observed experimentally because of insufficient resolution. Coupled channel scattering calculations (*16*) predict three metastable states above the dissociation limit (~8000 cm^{-1}) in good agreement with the experimental observations.

The experimental spectrum for DCO is deceptively simple and consists of six features with the appearance of a single harmonic-oscillator spectrum with a frequency of roughly 900 cm^{-1}. This result is clearly fallacious, because DCO must have more vibrational levels than HCO because the frequencies are lower for the stretching and bending modes ($\omega_{CD} \approx \omega_{CH}/\sqrt{2}$ and $\omega_{DCO} \approx \omega_{HCO}/\sqrt{2}$). Indeed, the variational calculations predict 28 bound vibrational states in DCO that cluster in groups (Fig. 2); these states could not be resolved in the photodetachment experiment. The reason for this clustering is that a near 2:1:1 Fermi resonance exists among the harmonic normal modes (ω_{DCO} = 897 cm^{-1}, ω_{CD} = 2054 cm^{-1}, and ω_{CO} = 1861 cm^{-1}). This resonance results in very strong mixing of the normal modes, which, because of the low resolution of the experiment, produces a spectrum of roughly equally spaced clumps. Note that the states predicted above 7000 cm^{-1} were not observed because of unfavorable Franck-Condon factors.

Finally, we note that the calculations predict the existence of a high-energy isomer, HOC (DOC). Although this isomer is not stable with respect to dissociation to H + CO, it could be long-lived because a large potential barrier (~14 kcal/mol) separates it from the more stable fragments. Our vibrational calculations predict three states of HOC below the barrier to dissociation and seven for DOC.

Dynamical studies involving the HCO system. The overall success of the empirically adjusted ab initio PES described above in reproducing the observed vibrational spectra has motivated theoretical studies of a number of dynamical processes involving the HCO system. To determine the addition and dissociation rate constants at combustion temperatures, a statistical (RRKM) theory calculation has been performed (*13*). Statistical theories presume that a metastable adduct is formed, which then randomly dissociates or is stabilized by collision with a third body. The agreement between the theoretical and (recent) experimental rate constants at temperatures below 900 K is good; these results have been used together to predict the rate constant at combustion temperatures for which direct measurements are not available.

The randomization approximation of statistical theories is being tested in this simple reaction by exact quantum dynamics scattering calculations. The part of the scattering due to lingering in the well as a metastable HCO* produces resonances or abrupt changes in the scattering at energies at which such motion occurs (*15, 16*)—this may be viewed as the temporary formation of metastable vibrational states. These resonances are being used to characterize (*23*) the quantum dynamics involving HCO* and thus permit a direct test of the statistical theories. The calculations are very computer-intensive because they require a large basis set to describe the wave function in the bound (well) region of the PES.

Classical trajectories calculations are also being used to characterize the behavior of H + CO collisions. Unlike quantum dynamics, which emphasizes the wave nature of atoms, classical mechanics

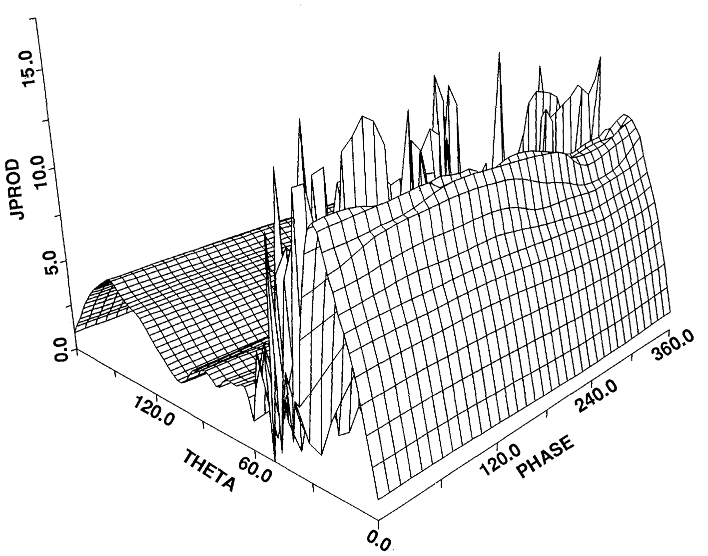

Fig. 3. The calculated final rotational angular momentum state JPROD of CO versus the initial rotational angle THETA and initial vibrational PHASE of CO in its ground rotational and vibrational state for the collision H + CO at a total energy of 5.47 kcal/mol (from an unpublished classical trajectory study by R. Steckler and A. F. Wagner).

treats atoms as particles and thus provides a means of correlating the dynamics of the system with the features of the PES. The level of detail that such studies can provide is shown in Fig. 3, which presents the final rotational angular momentum of CO produced by a collision of H with CO. In this study the total angular momentum of the collision complex and the initial rotational angular momentum of the CO are zero. The high, smooth peak in the foreground corresponds to trajectories that strike the carbon end of the CO at angles too near collinear to form the bent HCO. The smooth, low peak in the background corresponds to trajectories that strike the oxygen end of the CO. The choppy middle band shows the chaotic distribution that results from trajectories that form HCO*. The curvature of the surface near the carbon and oxygen atoms so evident in Fig. 1 produces the torque during the collision that gives rise to the above distributions. Actual experimental measurements would average over the angles seen in Fig. 3 but such averaging would still predict a bimodal distribution reflecting the consequences of collisions with either the oxygen or carbon atoms.

The OH + H_2 Reaction

The reaction between OH and H_2

$$OH + H_2 \rightarrow H_2O + H \qquad (1)$$

is important in many chemical processes, including combustion and atmospheric chemistry. This reaction is one of the three chain-carrying reactions in the oxidation of hydrogen and is the primary source of water produced in hydrogen and hydrocarbon flames (*24*). The OH radical is the dominant radical in the atmosphere and chemical removal of molecular hydrogen is mainly by the OH + H_2 reaction (*25*). Because of its pivotal role, this reaction has received and continues to receive attention by experimentalists and theoreticians alike (Table 1); it is, in fact, the best characterized four-body reaction to date.

Determination of a global potential energy surface for OH + H_2. It is not possible to determine a global PES for the OH + H_2 system as was done for the H + CO system—calculations at more than one million geometries would be required. Instead, we used the general form of the four-body PES advanced by Murrell and co-workers (*26*) and adjusted the parameters in this function (*27*) to agree with data from ab initio calculations (*28*). This procedure provides a means of smoothly interpolating from known data on the reactants, products, and transition state to a global PES. Although this PES does not precisely fit the ab initio calculations, it does accurately describe a number of features of the reaction dynamics.

Reaction path analysis of the global OH + H_2 *potential surface.* Although the PES clearly influences the dynamics of a reaction, the connection between the features of the PES and the reaction dynamics are often not obvious. The complexity of molecular PESs prevents their ready analysis and visualization. The connection between the features of PESs and the dynamics of reactions has, however, been a topic of keen interest since the 1930s. For example, Polanyi and Wong in the late 1960s (*29*) found that for highly exoergic reactions the barrier to reaction was early, that is, the geometry of the complex at the barrier most resembled the reactants, and, as a consequence, translational energy was most effective in enhancing the rate of reaction. Conversely, for endoergic reactions with late barriers, vibrational energy was found to be most effective in increasing the reaction (see also *30*).

A solid theoretical foundation for delineating the connection between the features of PESs and chemical reaction dynamics was put forward by Miller, Handy, and Adams in 1980 (*31*). These authors transformed the molecular Hamiltonian from internal coordinates, $\{x_i, i = 1,3N - 6\}$, to a set of reaction path coordinates, namely, $x_s(s)$, the reaction path, and $\{Q_i(s)\}$, the $(3N - 7)$ vibrational modes transverse to the reaction path, where s is the distance along the reaction path. The path chosen was the steepest descent path starting at the top of the barrier and leading to reactants in one direction and products in the other. This approach provides a description of the PES in terms of a harmonic reaction valley leading from reactants over the barrier to products. The meandering of the

Table 1. Summary of theoretical studies of the dynamics of the OH + H_2 and H + H_2O reactions.

Process	Methods	Summary of results
OH + H_2 Thermal rates	TST (*40*) QCT (*37*)	$k_{TST}(T)$ and $k_{QCT}(T)$ in good agreement with experiment.
	VTST (*50*)	$k_{VTST}(T)$ agrees with experiment within a factor of 1.7 over the range 298 to 2400 K.
OH(v,j) + $H_2(v',j')$ State-resolved rates*	QCT (*37*)	OH vibrational excitation has little effect on the rate, whereas
	VTST (*51*)	H_2 vibrational excitation enhances the rate by >100.
	QCT (*52, 53*)	OH and H_2 rotational excitation can both enhance and suppress reactivity.
H + H_2O Thermal and state-resolved rates	QCT (*38, 54*)	$k_{QCT}(T)$ in agreement with experiment. Asymmetric stretch excitation less effective than symmetric stretch in promoting reaction.
H + H_2O Hot hydrogen cross sections and product state distributions	QCT (*38, 54*)	Experimental cross section and OH rotational distribution agrees with theoretical prediction.

*(v,j) refer to vibrational and rotational states, respectively.

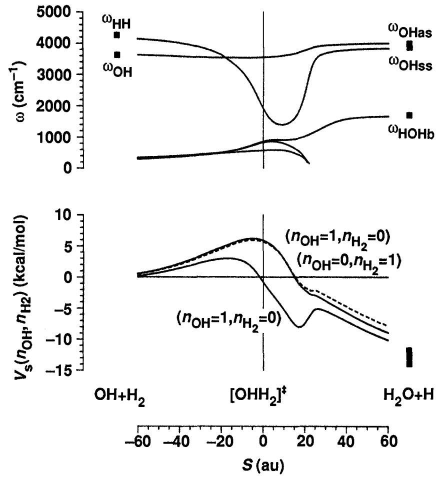

Fig. 4. Variation of the vibrational frequencies (upper panel) and vibrationally adiabatic potentials (lower panel) along the reaction path for the OH + H_2 reaction. The black squares denote the calculated vibrational frequencies for the reactants and product (upper panel) or the calculated reaction exoergicities (lower panel).

floor of the reaction valley is determined by the path, $x_s(s)$, whereas the inclination of the floor is determined by $V_0(s)$. The width of the reaction valley is determined by the vibrational frequencies, $\{\omega_k(s)\}$: low frequencies correspond to wide valleys, high frequencies to narrow valleys.

From an analysis of the terms in the reaction path Hamiltonian, a rationale can be provided for many of the qualitative features of reaction dynamics. For example, insight into the effect of vibrational excitation on the rates of chemical reactions can be gained by considering the vibrationally adiabatic potentials (VAPs). The VAPs are obtained by adding the change in the vibrational energy to the classical potential. If the frequency of one (or more) of the modes decreases significantly as the reaction proceeds, vibrational excitation of this mode will lead to a reduction in the vibrationally adiabatic barrier for the reaction and a corresponding increase in the reaction rate. The vibrational frequencies and vibrationally adiabatic potentials obtained from an analysis of the global PES discussed above are plotted in Fig. 4 (*32*).

The H_2 frequency drops dramatically as the reactants approach along the reaction path; this mode is strongly coupled to the reaction coordinate. The OH frequency varies little from reactants to the transition state; it is a spectator mode. The net result of these changes is that vibrational excitation of the OH radical decreases the vibrationally adiabatic barrier for the reaction by only 0.3 kcal/mol, whereas excitation of the H_2 molecule decreases the barrier by 3.0 kcal/mol (see Fig. 4). The decreases in the vibrationally adiabatic barriers increase the rate of reaction at 300 K by a factor of 1.6 for vibrationally excited OH and by a factor of nearly 150 for vibrationally excited H_2. These predictions agree well with the available experimental data. Zellner and Steinert (*33*) report that the rate of the OH + H_2 reaction at 300 K is increased by a factor of 120 ± 40 by vibrational excitation of H_2, whereas Glass and Chaturvedi (*34*) report an increase of 155 ± 38. In contrast, Spencer *et al.* (*35*) found that vibrational excitation of the OH increased the rate by less than a factor of 2; see also (*36*).

Furthermore, by explicitly considering the dynamical terms in the reaction path Hamiltonian (*31, 32*), even more detailed aspects of the dynamics of the OH + H_2 reaction, including the state-specific deposition of the excess vibrational excitation energy into the modes of water (*37*), can be understood.

Dynamical studies of the OH + H_2 *and H +* H_2O *reactions.* The above PES has been used to calculate a large number of dynamical properties of both the OH + H_2 reaction and the H + H_2O reverse reaction (*38*) (Table 1). The methods used include: (i) the quasiclassical trajectory method (QCT), which is a variant on the classical trajectory approach in which the initial and final states are determined by semiclassical methods, and (ii) conventional TST and its variational variant (VTST).

As indicated in Table 1, the thermal rate coefficients obtained from QCT and VTST are in excellent agreement with experiment (*39*) over a wide range of temperatures; see also (*40*). Since QCT and VTST are quite different methods, it may be surprising that the results agree well, but this often (but not always) happens in part because of canceling errors. QCT leaves out tunneling, which should result in lower rate constants, but trajectories tend to surmount barriers more easily than they should by shuffling energy from the modes perpendicular to the reaction path into reaction path motion. QCT does describe barrier recrossing effects that VTST leaves out, but this is relatively unimportant for OH + H_2.

A better test of the PES and dynamical methods is provided by considering state-resolved rate constants. The results obtained from both QCT and VTST calculations are in good agreement with those deduced from the reaction path analysis described above and the experimental measurements (*33–36*). Although the VTST assumes vibrational adiabaticity and QCT does not, the different effects of OH and H_2 excitation are still well reproduced.

A number of other properties of the OH + H_2 and H + H_2O reaction have been studied by using QCT methods. OH and H_2 rotational excitation can either enhance or suppress the OH + H_2 reaction rate depending on how much excitation is involved (Table 1). Rate constants for H + H_2O in a variety of vibrational states have been predicted, and several surprising mode-specific enhancements have been observed; again, the reaction path analysis provides a rationale for these results (*32*). To date, no experiments have been done to test these predictions, but one prediction that was subsequently tested concerns the influence of translational excitation on the cross section for H + H_2O. Recent work by Kleinermanns and Wolfrum (*41*) measured a cross section of $0.9a_0^2$ (a_0 is the Bohr radius) at a translational energy of 2.5 eV. This agrees with the earlier prediction of Elgersma and Schatz (*38*) that the cross section would be $\sim 1.0a_0^2$. Measured OH rotational distributions are also in good agreement with the trajectory calculations.

The O + C_2H_2 Reaction

The reactions of acetylene are an integral part of the overall mechanism for the oxidation of many hydrocarbon species, including methane. From modeling studies of both flame and shock tube experiments, Miller and co-workers (*42*) concluded that the reactions of atomic oxygen with acetylene

$$O + C_2H_2 \rightarrow OC_2H_2^* \rightarrow H + HC_2O \qquad (2a)$$

$$\rightarrow CH_2 + CO \qquad (2b)$$

"are the most important fuel consuming reaction under lean, stoichiometric, and even slightly rich conditions." Further, they noted that in spite of numerous experimental studies "[t]he branching ratio between the two sets of products is still a source of uncertainty." In fact, many early attempts to model hydrocarbon flames simply assumed that the thermodynamically most stable product, CH_2 + CO, was formed in reaction 2. Here we summarize our theoretical studies of reactions 2a and 2b and focus on the role that these studies have played in quantifying the branching ratio for this reaction. The theoretical studies provided strong evidence that 2a was a significant pathway and led to further experimental studies of this important reaction.

Characterization of the critical regions of the O + C_2H_2 *PES.* It is not possible to map out either a global PES or detailed reaction paths for the O + C_2H_2 reaction with standard ab initio electronic structure methods. For this reason the electronic structure calculations were limited to the critical regions of the PES, namely, those corresponding either to minima (reactants, products, or bound intermediates) or saddle points (transition states connecting one stable species with another). Each such point was characterized by determining its energy, geometry, and harmonic vibrational frequencies (*43*).

The relative energies of the stable species and transition states are summarized schematically in Fig. 5. There are three electronic surfaces involved in this reaction, corresponding to the three different orientations of the singly and doubly occupied oxygen *p* orbitals relative to the acetylene. Reaction can occur on two of these surfaces. On the lowest surface, the $^3A''$ surface, the oxygen radical orbitals are oriented in such a way as to attack both acetylene π bonds. The resulting adduct then has a carbon-oxygen double bond, a carbon-carbon single bond, and a carbene center. Addition on the upper reactive surface, the $^3A'$ surface, results in the disruption of only one acetylene π bond leading to a biradical structure with a carbon-oxygen single bond and a carbon-carbon double bond. The $^3A''$ surface is lower in energy primarily because a carbon-carbon π bond is replaced by a stronger carbon-oxygen π bond.

Once formed, the $^3A''$ adduct can decay either by carbon-hydrogen bond rupture, forming the ketyl radical (2a):

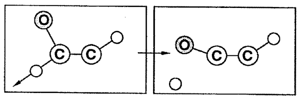

or by a (1,2)-hydrogen migration, forming triplet ketene followed by carbon-carbon bond rupture to yield methylene and carbon monoxide (2b):

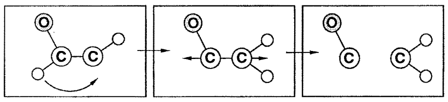

Because the latter decomposition process is quite exothermic, the branching ratio for this reaction is determined by the relative rates of CH bond rupture versus hydrogen migration. The calculations predict that the transition states for these two processes lie very close in energy. The most significant difference between the two transition states is that the transition state for bond rupture is much looser than that for migration, that is, at the transition state for CH bond rupture the leaving hydrogen atom is far from the ketyl radical, the H–OC_2H interactions are weak, and the reaction valley is wide (low-frequency vibrational modes). The reaction therefore favors pathway 2a.

Dynamical studies of the branching ratio of the O + C_2H_2 reaction. The branching ratio is defined as the ratio of the rate of production of H + HC_2O (k_{2a}) relative to the overall rate of loss of O ($k = k_{2a} + k_{2b}$). Given the above information, this branching ratio can be calculated with RRKM theory. RRKM theory provides accurate predictions of branching ratios when long-lived adducts are involved, and OCHCH* is known to have a lifetime that exceeds its rotational period (*44*).

The calculated value of the branching ratio as a function of temperature is compared to experimental measurements (*45–47*) in Fig. 6. There were four additional measurements (*48*) that concluded that the branching ratio at room temperature was substantial, but were unable to determine its value. The calculated branching ratio is ~70% and essentially independent of temperature. The lack of temperature dependence is because the barrier to dissociation of the OC_2H_2* adduct to either product is substantially below the barrier to adduct formation (see Fig. 5). Thus the adduct always has sufficient energy to dissociate to either product (*49*). Although the size of the branching ratio depends on the precise differences in the energies and properties of the two saddle points and thus cannot be predicted with great accuracy at present, the reduced steric hindrance (wide reaction valley) at the saddle point for hydrogen atom dissociation relative to hydrogen atom migration causes the branching ratio to favor dissociation.

Fig. 5. Relative energies of the reactants, products, bound intermediates, and transition states for the O + C_2H_2 reaction on both the $^3A'$ and $^3A''$ surfaces.

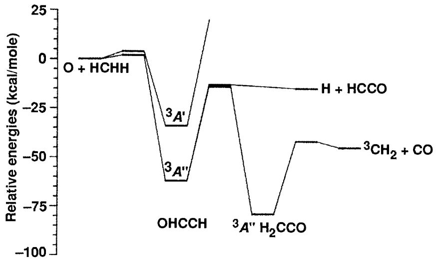

Fig. 6. Comparison of theory and experiment for the branching ratio of the O + C_2H_2 reaction [the ratio of the rate of production of H + HC_2O, (k_{2a}), to the overall rate of loss of O by reaction with C_2H_2, ($k_{2a} + k_{2b}$)]. The solid line is the calculated curve. The dashed and dotted lines are the most recent measurements reported in (*47*) and (*48*). The symbols are the earlier measurements listed in (*46*).

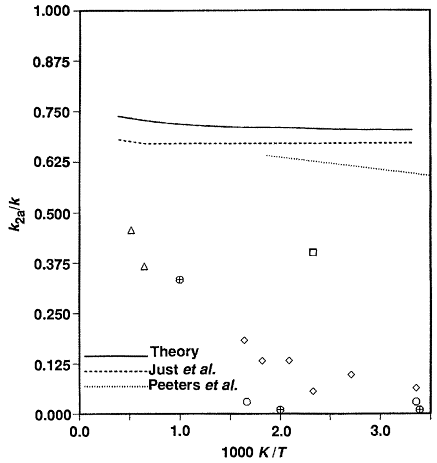

We must note that the majority of the measurements in Fig. 6 disagree with these conclusions. These measurements led to the adoption of a low value for the branching ratio in many kinetics models of acetylenic flames. However, the two most recent measurements (*46, 47*), that were performed during or after the calculations, are in substantial agreement with the above prediction. In fact, the most recent kinetics model for acetylenic flames (*42*) incorporates a temperature-independent branching ratio of 0.5; this model reproduces all of the known properties of the flame.

Conclusion

The applications discussed in this article show that even relatively simple chemical reactions are rich in dynamical detail once we have the theoretical methods and computational resources available to study them. In a few cases, theoretical methods were able to predict results that stimulated new experimental studies, but more often we used our results to interpret confusing or conflicting experimental data and to provide insight as to why certain results were obtained and how general the conclusions were. Although all of the systems that we considered are ones for which extensive experimental studies are possible, one of the most valuable roles of theory in the future promises to be in characterizing reactions that are difficult to study experimentally, such as reactions between radicals, or reactions involving unstable molecules and molecules in excited states. The level of accuracy that can be provided by ab initio electronic structure calculations of the type that we reported here is currently limited to reactions involving a relatively small number of atoms (three to six), but the continuing development of new computer hardware and software, along with fundamental advances in chemical theory, promise to greatly expand this number in the not too distant future.

REFERENCES AND NOTES

1. R. Shepard *et al.*, *Int. J. Quantum Chem. Symp.* **17**, 613 (1983); R. A. Bair and T. H. Dunning, Jr., *J. Comput. Chem.* **5**, 44 (1984).
2. I. Shavitt, *Int. J. Quantum Chem. Symp.* **12**, 5 (1978); B. R. Brooks, W. D. Laidig, P. Saxe, N. C. Handy, H. F. Schaefer III, *Phys. Scr.* **21**, 312 (1980); P. E. M. Siegbahn, *J. Chem. Phys.* **72**, 1647 (1980); H. Lischka, R. Shepard, F. B. Brown, I. Shavitt, *Int. J. Quantum Chem. Symp.* **15**, 91 (1981).
3. For a review of this work, see R. J. Bartlett, *Annu. Rev. Phys. Chem.* **32**, 359 (1981) (a review in preparation is contained in R. J. Bartlett, "Coupled cluster methods for the structure and spectra of molecules," *Computer Physics Reports*, in press).
4. J. A. Pople, R. Krishnan, H. B. Schlegel, J. S. Binkley, *Int. J. Quantum Chem. Symp.* **13**, 225 (1979); R. Krishnan, H. B. Schlegel, J. A. Pople, *J. Chem. Phys.* **72**, 4654 (1980); Y. Osamura, Y. Yamaguchi, H. F. Schaefer III, *ibid.* **75**, 2919 (1981); *ibid.* **77**, 383 (1982); D. J. Fox *et al.*, *Chem. Phys. Lett.* **102**, 17 (1983).
5. For a review of this work, see H. F. Schaefer III, *J. Chem. Phys.* **89**, 5336 (1985).
6. M. J. Frisch *et al.*, *Chem. Phys. Lett.* **114**, 1 (1985).
7. R. Steckler, D. W. Schwenke, F. B. Brown, D. G. Truhlar, *ibid.* **121**, 475 (1985); D. W. Schwenke, R. Steckler, F. B. Brown, D. G. Truhlar, *J. Chem. Phys.* **86**, 2443 (1987).
8. C. W. Bauschlicher, S. P. Walch, S. R. Langhoff, P. R. Taylor, R. L. Jaffe, *J. Chem. Phys.* **88**, 1743 (1988).
9. K. K. Baldridge, J. A. Boatz, S. Koseki, M. S. Gordon, *Annu. Rev. Phys. Chem.* **38**, 211 (1987).
10. S. Chu and A. Dalgarno, *Proc. R. Soc. London* **342**, 194 (1975); S. Green and P. Thaddeus, *Astrophys. J.* **205**, 766 (1976).
11. G. Caracciolo *et al.*, *Astrophys. J.* **229**, 451 (1979).
12. J. F. McKellar and R. G. W. Norrish, *Proc. R. Soc. London Ser. A* **254**, 147 (1960); D. J. Seery and C. T. Bowman, *Combust. Flame* **14**, 37 (1970); H. Y. Wang, J. A. Eyre, L. M. Dorfman, *J. Chem. Phys.* **59**, 5199 (1973).
13. R. S. Timonen, E. Ratajczak, D. Gutman, A. F. Wagner, *J. Phys. Chem.* **91**, 5325 (1987).
14. A. F. Wagner and J. M. Bowman, *ibid.*, p. 5314.
15. H. Romanowski, K.-T. Lee, J. M. Bowman, L. B. Harding, *J. Chem. Phys.* **84**, 4888 (1986).
16. K.-T. Lee and J. M. Bowman, *ibid.* **85**, 6225 (1986); *ibid.* **86**, 215 (1987).
17. C. F. Wood, G. W. Flynn, R. E. Weston, Jr., *ibid.* **77**, 4776 (1982); C. A. Wight and S. R. Leone, *ibid.* **78**, 4875 (1983); *ibid.* **79**, 4823 (1983); G. K. Chawla, G. McBane, P. L. Houston, paper presented at the Conference on the Dynamics of Molecular Collisions, 12 to 17 July 1987, Wheeling, WV.
18. L. C. Geiger and G. C. Schatz, *J. Phys. Chem.* **88**, 214 (1969); L. C. Geiger, G. C. Schatz, L. B. Harding, *Chem. Phys. Lett.* **114**, 520 (1985).
19. D. E. Milligan and M. E. Jacox, *J. Chem. Phys.* **51**, 277 (1969); P. Warneck, *Z. Naturforsch. Teil A* **29**, 350 (1974); B. M. Stone, M. Noble, E. K. C. Lee, *Chem. Phys. Lett.* **118**, 83 (1985).
20. K. K. Murray, T. M. Miller, D. G. Leopold, W. C. Lineberger, *J. Chem. Phys.* **84**, 2520 (1986).
21. J. M. Bowman, J. S. Bittman, L. B. Harding, *ibid.* **85**, 911 (1986); K. M. Christoffel, J. S. Bittman, J. M. Bowman, *Chem. Phys. Lett.* **133**, 525 (1987).
22. S. R. Langhoff and E. R. Davidson, *Int. J. Quantum Chem.* **8**, 61 (1974); E. R. Davidson and D. W. Silver, *Chem. Phys. Lett.* **52**, 403 (1978).
23. J. M. Bowman, *J. Phys. Chem.* **90**, 3492 (1986).
24. N. J. Brown, K. H. Eberius, R. M. Fristrom, K. H. Hoyermann, H. Gg. Wagner, *Combust. Flame* **33**, 151 (1978).
25. J. Heicklen, *Atmospheric Chemistry* (Academic Press, New York, 1976).
26. For a discussion of this technique, see J. N. Murrell, *Gas Kinetics and Energy Transfer*, P. G. Ashmore and R. J. Donovan, Eds. (The Chemical Society, London, 1978), vol. 3, pp. 200–222.
27. G. C. Schatz and H. Elgersma, *Chem. Phys. Lett.* **73**, 21 (1980).
28. S. P. Walch and T. H. Dunning, Jr., *J. Chem. Phys.* **72**, 1303 (1980).
29. J. C. Polanyi and W. H. Wong, *ibid.* **51**, 1439 (1969).
30. For a review of this and related work, see D. G. Truhlar and D. A. Dixon, *Atom-Molecule Collision Theory. A Guide for the Experimentalist*, R. B. Bernstein, Ed. (Plenum, New York, 1979), pp. 595–646.
31. W. H. Miller, N. C. Handy, J. E. Adams, *J. Chem. Phys.* **72**, 99 (1980).
32. T. H. Dunning, Jr., E. Kraka, R. A. Eades, *Faraday Discuss. Chem. Soc.*, in press.
33. R. Zellner and W. Steinert, *Chem. Phys. Lett.* **81**, 568 (1981).
34. G. P. Glass and B. K. Chaturvedi, *J. Chem. Phys.* **75**, 2749 (1981).
35. J. E. Spencer, H. Endo, G. P. Glass, *Sixteenth Symposium (International) Combustion* (The Combustion Institute, Pittsburgh, 1977), p. 829.
36. G. C. Light and H. Matsumoto, *Chem. Phys. Lett.* **58**, 578 (1978).
37. G. C. Schatz, *J. Chem. Phys.* **74**, 1133 (1981).
38. H. Elgersma and G. C. Schatz, *Int. J. Quant. Chem. Symp.* **15**, 611 (1981).
39. I. W. M. Smith and R. Zellner, *J. Chem. Soc. Faraday Trans. 2*, **70**, 1045 (1974); F. P. Tully and A. R. Ravishankara, *J. Phys. Chem.* **84**, 3126 (1980); P. Frank and Th. Just, *Ber. Bunsenges. Phys. Chem.* **89**, 181 (1985); see also S. Madronich and W. Felder, *J. Phys. Chem.* **88**, 1857 (1984); J. V. Michael and J. W. Sutherland, *ibid.*, in press.
40. G. C. Schatz and S. P. Walch, *J. Chem. Phys.* **72**, 776 (1980).
41. K. Kleinermanns and J. Wolfrum, *Appl. Phys. B* **34**, 5 (1984).
42. J. A. Miller, R. E. Mitchell, M. D. Smooke, R. J. Kee, *Nineteenth Symposium (International) on Combustion* (The Combustion Institute, Pittsburgh, 1982), p. 181.
43. L. B. Harding, *J. Phys. Chem.* **85**, 10 (1981); L. B. Harding and A. F. Wagner, *ibid.* **90**, 2974 (1986).
44. A. R. Clemo, G. L. Ducan, R. Grice, *J. Chem. Soc. Faraday Trans. 2* **78**, 1231 (1982); *ibid.* **79**, 637 (1983).
45. E. N. Aleksandrov, U. S. Arutyunov, S. N. Kozlov, *Kinet. Catal.* **22**, 391 (1981); R. Lohr and P. Roth, *Ber. Bunsenges. Phys. Chem.* **85**, 153 (1981); D. G. Williamson, *J. Phys. Chem.* **75**, 4053 (1971); B. Blumenberg, K. Hoyermann, R. Sievert, *Sixteenth Symposium (International) on Combustion* (The Combustion Institute, Pittsburgh, 1977), p. 841; K. H. Homann and H. Schweinfurth, *Ber. Bunsenges. Phys. Chem.* **85**, 569 (1981); K. H. Homann and Ch. Wellmann, *ibid.* **87**, 609 (1983).
46. K. A. Bhaskaaran, P. Frank, Th. Just, *Twenty-first Symposium (International) on Combustion* (The Combustion Institute, Pittsburgh, in press).
47. J. Peeters, M. Schaekers, C. Vinckier, *J. Phys. Chem.* **90**, 6552 (1986).
48. D. G. Williamson and K. D. Bayes, *ibid.* **73**, 1232 (1969); I. T. N. Jones and K. D. Bayes, *Fourteenth Symposium (International) on Combustion* (The Combustion Institute, Pittsburgh, 1973), p. 277; J. R. Kanofsky, D. Lucas, F. Pruss, D. Gutman, *J. Phys. Chem.* **78**, 311 (1974); C. Vinckier, M. Schaekers, J. Peeters, *ibid.* **89**, 508 (1985).
49. Despite the excess energy, the calculations do show adduct lifetimes that exceed one rotational period, as required by the molecular beam results.
50. A. D. Isaacson and D. G. Truhlar, *J. Chem. Phys.* **76**, 1380 (1982); A. D. Isaacson, M. T. Sund, S. N. Rai, D. G. Truhlar, *ibid.* **82**, 1338 (1985).
51. D. G. Truhlar and A. D. Isaacson, *ibid.* **77**, 3516 (1982).
52. O. Rashed and N. J. Brown, *ibid.* **82**, 5506 (1985).
53. J. A. Harrison and H. R. Mayne, *ibid.* **87**, 3698 (1987).
54. G. C. Schatz, M. C. Colton, J. L. Grant, *J. Phys. Chem.* **88**, 2971 (1984).
55. T.H.D. thanks his co-workers whose efforts over the past decade have significantly contributed to the above research program: S. P. Walch, R. A. Bair, R. A. Eades, and E. Kraka. We also thank R. M. Pitzer, I. Shavitt, R. A. Bair, and R. L. Shepard, without whose skills in developing and implementing new techniques for solving the electronic Schrödinger equation, this (and future) work would not be possible. This work was performed under the auspices of the Division of Chemical Sciences, Office of Basic Energy Sciences, U.S. Department of Energy under contract W-31-109-Eng-38.